Recent Progress in the Numerical Simulation Reactor Research Project*)

Hideo SUGAMA[1,2)] and the Numerical Simulation Reactor Research Project Group[1)]

[1)]*National Institute for Fusion Science, National Institutes of Natural Sciences, Toki 509-5292, Japan*

[2)]*Department of Fusion Science, SOKENDAI (The Graduate University for Advanced Studies), Toki 509-5292, Japan*

(Received 27 December 2018 / Accepted 12 February 2019)

Fusion plasmas are complex systems which involve a variety of physical processes interacting with each other across wide ranges of spatiotemporal scales. In the National Institute for Fusion Science (NIFS), we are utilizing the full capability of the supercomputer (Plasma Simulator) and propelling domestic and international collaborations in order to conduct the Numerical Simulation Reactor Research Project (NSRP). Understanding physical mechanisms of complex plasma phenomena for the systematization of fusion science, NSRP aims at realization of the Numerical Helical Test Reactor, which is an integrated system of simulation codes to predict behaviors of fusion plasmas over the whole machine range. In NSRP, eight task groups are organized to cover a wide range of fusion simulation subjects: plasma fluid equilibrium stability, energetic-particle physics, integrated transport simulation, neoclassical and turbulent transport simulation, peripheral plasma transport, plasma-wall interaction, multi-hierarchy physics, and simulation science basis. Verification and validation researches are in progress in these task groups collaborating with each other as well as with experimental and engineering groups. Successful examples of validations of large-scale simulations of energetic particle driven instabilities and neoclassical and turbulent transport against experimental results from tokamaks and helical systems are highlighted. In addition, recent achievements in advanced simulation studies on ion heating processes and plasma-wall interactions, as well as those in the application of Virtual-Reality (VR) technology to fusion engineering, are presented.

Keywords: numerical simulation, fusion plasma, helical system, tokamak, instability, transport, virtual reality

DOI: 10.1585/pfr.14.3503059

1. Introduction

Based on past research activities in large-scale numerical simulations, the Numerical Simulation Research Project [1] was launched in 2010 to continue their tasks and develop them in more systematic ways on the occasion of the re-organization of the National Institute for Fusion Science (NIFS). The project was renamed as the Numerical Simulation Research Reactor Project (NSRP) [2] in order to accelerate the research activity towards the construction of the Numerical Helical Test Reactor in 2014. Missions of the NSRP are i) to systematize understandings of physical mechanisms in fusion plasmas for making fusion science a well-established discipline and ii) to construct the Numerical Helical Test Reactor, which is an integrated system of simulation codes to predict behaviors of fusion plasmas over the whole machine range.

To fulfill the missions of the NSRP, the supercomputer system Plasma Simulator has been made full use of. The Plasma Simulator was replaced by Fujitsu PRIMEHPC FX100 with the total peak performance of 2.62 Petaflops, and the total main memory of 81TB as of 2015. The snap shot of the Plasma Simulator, PRIMEHPC FX100, is shown in Fig. 1. The Plasma Simulator is widely utilized not only for NSRP but also for numerical simulation studies done by many researchers in plasma physics and fusion science. Figure 2 shows progress in the peak performance of the Plasma Simulator and the number of submitted jobs per month in past years.

Fig. 1 The Plasma Simulator, PRIMEHPC FX100.

The structure of NSRP is shown in Fig. 3. In 2017, Prof. Ritoku Horiuchi, the Executive Director of NSRP, was succeeded by Hideo Sugama. The Plasma Simulator Working Group makes management of the supercomputer system for efficiently performing simulation research. The steering committee consists of the Executive

author's e-mail: sugama@nifs.ac.jp

*) This article is based on the plenary presentation at the 27th International Toki Conference (ITC27) & the 13th Asia Pacific Plasma Theory Conference (APPTC2018).

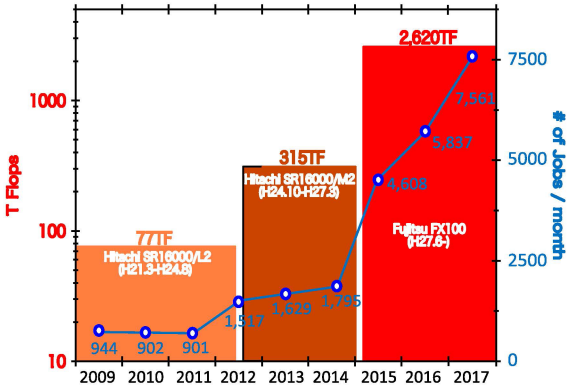

Fig. 2 Progress in the peak performance of the Plasma Simulator and the number of submitted jobs per month from 2009 to 2017.

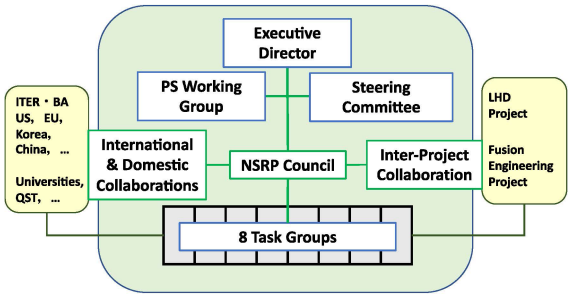

Fig. 3 The structure of the Numerical Simulation Research Reactor Project (NSRP).

Director, leaders of eight task groups, and directors of two divisions, namely, the Fusion Theory and Simulation Research Division and the Fundamental Physics Simulation Research Division in NIFS. All project members work in some of the task groups and participate in the NSRP Council to discuss research plans carried out through collaborations with domestic and foreign institutions as well as collaborations with the Large Helical Device (LHD) Project [3] and the Fusion Engineering Research Project [4] in NIFS.

The eight task groups are organized to cover a wide range of fusion simulation subjects: plasma fluid equilibrium stability [5], energetic-particle physics [6], integrated transport simulation [7], neoclassical and turbulent transport simulation [8], peripheral plasma transport [9], plasma-wall interaction [9], multi-hierarchy physics [10], and simulation science basis [10]. Leaders and numbers of members of the eight task groups are shown in Fig. 4. Each task group has from about 10 to 20 members. Many collaborators from other projects in NIFS and from other universities and institutions have joined these task groups to enhance collaboration and cooperation studies. Most of the simulation staff members of each task group also participate in other task groups.

In the rest of this Overview, highlights of recent achievements accomplished in NSRP are presented. In

group	leader	member
Plasma fluid equilibrium stability	K. Ichiguchi	13（sim. 7, exp. 3, collab. 3）
Energetic-particle physics	Y. Todo	8（sim. 3, exp. 3, collab. 2）
Integrated transport simulation	M. Yokoyama	28（sim. 4, exp. 13, collab. 11）
Neoclassical and turbulent transport simulation	R. Kanno	15（sim. 8, exp. 2, collab. 5）
Peripheral plasma transport	Y. Suzuki	20（sim. 4, exp. 5, collab. 11）
Plasma-wall interaction	H. Nakamura	17（sim. 3, exp. 3, collab. 11）
Multi-hierarchy physics	H. Miura	18（sim. 12, collab. 6）
Simulation science basis	H. Ohtani	16（sim. 12, exp. 1, collab. 3）

Sim.: simulation staff, exp.:experiment staff, collab.:domestic collaborators

Fig. 4 The eight task groups in the Numerical Simulation Research Reactor Project (NSRP). Leaders and numbers of members of the eight task groups are shown.

Sec. 2, recent results from kinetic and magnetohydrodynamic (MHD) hybrid simulations of energetic particle driven instabilities are shown. Next, neoclassical and turbulent transport studies based on drift kinetic and gyrokinetic simulations are explained in Sec. 3, where developments in turbulent transport modeling and an integrated transport code are described, as well. Results from some of the other research activities in our project, such as particle simulations of ion heating processes in spherical tokamaks, multi-hybrid simulations of fuzzy structures on a tungsten surface, and application of Virtual-Reality (VR) technology to fusion engineering, are reviewed in Sec. 4. Finally, summary and future plans are given in Sec. 5.

2. Simulation Studies on Energetic Particle Driven Instabilities

Recent results from simulation studies on energetic particle (EP) driven instabilities are presented in this section. Alfvén eigenmodes (AEs) driven by alpha particles are one of the major concerns regarding the future burning plasmas because they can enhance alpha particle transport, reduce alpha particle heating efficiency, and deteriorate fusion reactor performance. For simulation studies on such EP driven instabilities, the MEGA code was developed by Todo [11]. Hybrid simulations for EPs and magnetohydrodynamics (MHD) are done by the MEGA code, in which EPs such as fast ions and alpha particles are treated by gyrokinetic Particle-in-cell (PIC) simulation and a bulk plasma by MHD simulation. The coupling between EPs and MHD is taken into account through the EP current in the MHD momentum equation. In addition, processes of neutral beam injection (NBI), EP collisions, and their losses are included in MEGA code simulations.

The MEGA code has been extensively applied to study EP driven instabilities in tokamaks such as ITER [12], DIII-D [13], JT-60U [14], EAST [15], KSTAR [16], and AUG [17], as well as in stellarator/heliotron plasmas such as LHD [18] and Heliotron J [19]. Validations of MEGA code simulations have been performed on fast ion profile flattening and electron temperature fluctuations in

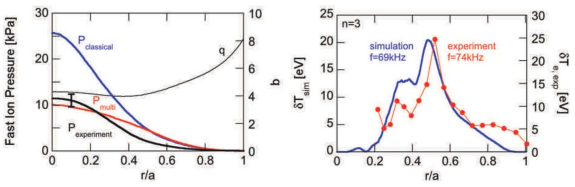

Fig. 5 Radial profiles of the fast ion pressure (left) and temperature fluctuations (right) obtained from the MEGA simulations and the DIII-D experiments (reproduced from Ref. [13] with the permission of the IAEA publishing section).

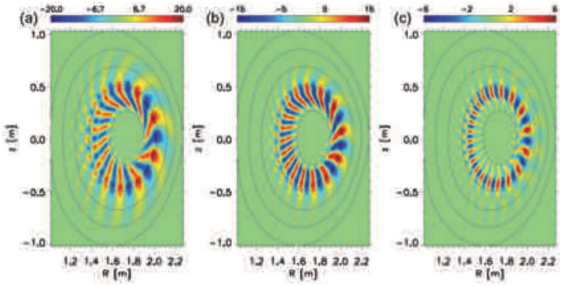

Fig. 6 The EP-driven TAE mode structures obtained from the simulations (reproduced from Ref. [13] with the permission of the IAEA publishing section).

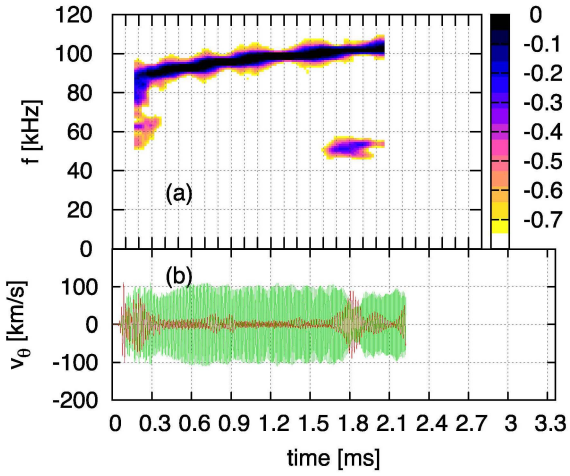

Fig. 7 The EGAMs in LHD reproduced by the MEGA code simulation (reproduced from Ref. [24] with the permission of the American Physical Society). (a) The poloidal velocity frequency spectrum including all of the frequency components. (b) The poloidal velocity time evolution including only 50 kHz (red) and 100 kHz (green).

DIII-D [13], Abrupt Large Events (ALEs) in JT-60U [14], and AE bursts in LHD [18]. Also, fast ion profile stiffness due to the resonance overlap of multiple Alfvén eigenmodes is verified by the MEGA simulation [20]. Good agreements between results from the MEGA simulations and those from the DIII-D experiment regarding radial profiles of fast ion pressure and temperature fluctuations are shown in Fig. 5. The EP-driven TAE mode structures obtained from the simulations are given in Fig. 6.

For another example, the MEGA code is used to simulate synchronization of multiple AEs and fast ion energy flux profile evolution observed in the TFTR experiment [21–23]. The simulation shows that the time interval of the bursts is about 3 ms and the maximum amplitude of the radial MHD fluid velocity normalized by the Alfvén velocity is given by $v_r/v_A \sim 3 \times 10^{-3}$, which are close to the results from the TFTR experiment. The simulation is performed for the input power 10 MW by NBI which is the same input power as in the TFTR experiment [23]. The fast ion energy flux was not experimentally found although the maximum fast ion energy flux shown by the simulation reaches 60 MW, which is six times larger than the input power. This large transport of fast ions caused by the multiple AEs implies a terrible deterioration of the NB heating efficiency as observed in the TFTR experiment [23]. Physical mechanisms of the synchronization of multiple AEs are elucidated by analyzing the time evolution of structures of the fast ion distribution function in the space of particle energy and the canonical toroidal momentum as follows. Before the AE burst, multiple AEs grow to low amplitudes and flatten the fast ion distribution function, which takes a stepwise form. When the stepwise distribution reaches a critical distribution, the further beam injection leads to broadening of the locally flattened regions and their overlap. Then, the overlap of locally flattened regions brings about synchronized sudden growth of AEs and global transport of fast ions. The MEGA simulation also confirms the profile resiliency which implies that almost the same fast ion pressure profile and distribution function are obtained for the beam powers of 5 MW and 10 MW.

Energetic particle driven geodesic acoustic modes (EGAMs) are experimentally observed in tokamaks and helical systems. Simulations are successfully performed using the MEGA code to investigate the EGAMs observed in the LHD experiments [24]. Figure 7 shows that the frequency chirping of the primary mode and the sudden excitation of the half-frequency secondary mode observed in LHD [25] are reproduced by the hybrid simulation using the realistic physical condition and the three-dimensional equilibrium. It is found from Figs. 7 (a) and (b) that the secondary mode which has a half frequency (50 kHz) of the primary mode frequency (100 kHz) is excited at $t \simeq 1.8$ ms by energetic particles satisfying the linear and nonlinear resonance conditions, respectively, for the primary and secondary modes [24]. Both EGAMs have global spatial profiles which are consistent with the experimental observations.

The bulk ion heating during the EGAM activity in LHD is also demonstrated for the first time by the MEGA simulation [26, 27]. The extended MEGA code which includes both kinetic EPs and kinetic thermal ions is devel-

oped to analyze EGAM physics such as energy channeling. It is found from the MEGA simulation that, when the EPs lose energy, the ions obtain energy through an energy channel established by the EGAM activity. The heating power found by the simulation is 3.4 kW/m^3, which is close to the value evaluated from the experiment.

Another interesting application of the extended MEGA code is stability analysis of LHD bulk plasmas. For high beta LHD plasmas which are unstable against the resistive ballooning modes, linear and nonlinear simulations using the extended MEGA code are performed. Then, the ion kinetic effects are found to reduce the linear growth rate of resistive ballooning modes [28]. Comparing nonlinear MHD and kinetic MHD simulation results shows that the nonlinear MEGA simulation result is more consistent with high beta LHD experiments than the MHD simulation in that the decrease of the central pressure for the former case is smaller than that for the latter one.

3. Simulation Studies on Neoclassical and Turbulent Transport

To understand and predict plasma confinement performance accurately, both neoclassical and turbulent transport processes need to be studied especially for helical systems. In this section, recent results from simulation studies on neoclassical and turbulent transport in NSRP using various drift kinetic and gyrokinetic simulation codes are described.

The gyrokinetic Vlasov (GKV) code was developed for Eulerian gyrokinetic simulation of turbulent transport using a local flux-tube spatial domain [29]. At first, model magnetic geometries of large-aspect-ratio toroidal systems were employed in the GKV code although it can now treat accurate magnetic configurations under the MHD equilibrium conditions corresponding to real experiments in tokamaks and helical systems. Validation of the GKV code simulation is successfully performed for a JT-60U L-mode plasma [30]. It is confirmed that the nonlinear GKV simulation can reproduce the experimental values of the ion and electron heat transport fluxes by varying temperature gradients within 30% from those observed in the experiment. In addition, the simulation shows that, in the core region, the ion temperature gradient (ITG) mode is a dominant instability while, in the edge region, the trapped electron mode (TEM) is dominant.

The GKV code is also applied to evaluate turbulent transport fluxes in the high ion temperature (T_i) LHD discharge (#88343) [31, 32]. The nonlinear GKV simulation using the flux tube located at the normalized minor radius $\rho = 0.65$ gives the turbulent electron energy flux which is in good agreement with the experimental observation. It is found from the simulation at $\rho = 0.65$ that the turbulent particle flux is directed radially inward [32]. It is also shown that when reducing the ion temperature gradient at $\rho = 0.65$ from the experimental value by 20% the turbulent ion heat flux given from the simulation agrees with the experimentally observed value [32]. In other words, the predicted temperature gradient deviates from experimental observation about 20%.

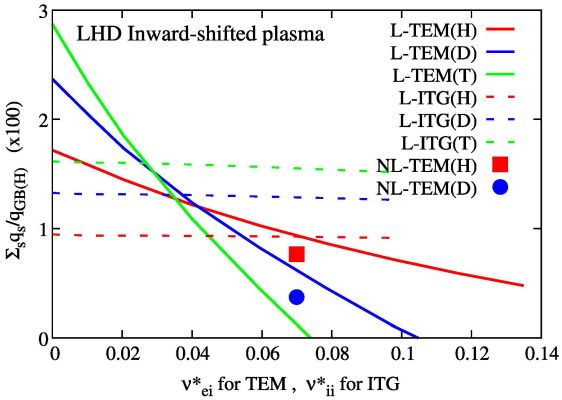

Fig. 8 Collisionality dependence of the radial heat flux $\sum_{s=i,e} q_s$ evaluated by the mixing-length diffusivity $\gamma/k_\perp^2$ for the linearTEM (L-TEM) and ITG (L-ITG) modes in the LHD inward-shifted hydrogen (H), deuterium (D), and tritium (T) plasmas (reproduced from Ref. [34] with the permission of the American Physical Society). For qualitative comparison, nonlinear TEM simulation results for the H and D cases [NL-TEM(H) and NL-TEM(D)] are also plotted.

In 2017, LHD deuterium experiments started. Investigation of isotope effects on plasma transport is one of the important subjects of the deuterium experiments. Prior to the LHD deuterium experiments, predictive studies with gyrokinetic simulations for isotope effects also started. Gyrokinetic TEM and ITG turbulence simulations in helical plasmas with hydrogen isotope ions and real-mass kinetic electrons are done using the GKV code [33, 34]. It is found from the simulation results that combined effects of the collisional TEM stabilization by the isotope ions and the associated increase in the impacts of the steady zonal flows at the near-marginal linear stability lead to the significant transport reduction. Figure 8 shows collisionality dependence of the radial heat flux $\sum_{s=i,e} q_s$ evaluated by the mixing-length diffusivity $\gamma/k_\perp^2$ for the linear TEM (L-TEM) and ITG (L-ITG) modes in the LHD inward-shifted hydrogen (H), deuterium (D), and tritium (T) plasmas. Nonlinear TEM simulation results for the H and D cases [NL-TEM (H) and NL-TEM (D)] are also plotted in Fig. 8. We see that collisional effects on stabilization of TEM and reduction of TEM turbulent transport are stronger for D plasmas than for H plasmas. In Fig. 8, nonlinear TEM simulation results for the heat fluxes in the LHD H and D plasmas are shown only for the single collisionality because the nonlinear GKV simulations for the LHD configuration need huge computational costs. Note that the heat fluxes obtained from nonlinear TEM simulations for H and D plasmas in the cyclone-base-case (CBC) like tokamak with different collisionalities are given by Fig. 4 of

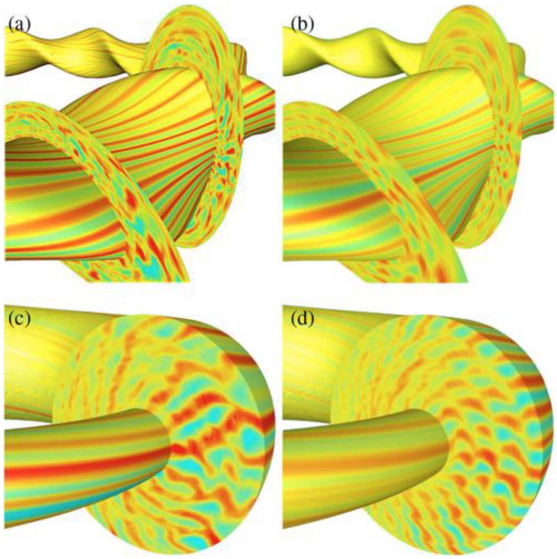

Fig. 9 Spatial structures of TEM potential fluctuations in hydrogen (H) and deuterium (D) plasmas in LHD and the CBC-like tokamak (reproduced from Ref. [34] with the permission of the American Physical Society). Turbulence simulation results for the H and D plasmas in LHD are shown in (a) and (b), respectively, while those for the tokamak H and D plasmas are in (c) and (d), respectively.

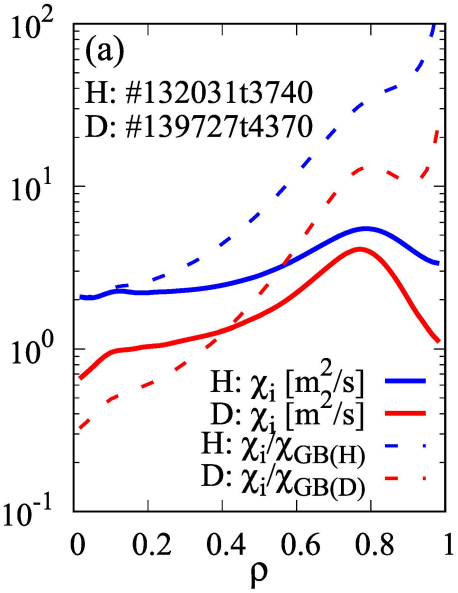

Fig. 10 Radial profiles of the ion heat diffusivities (χ_i's) evaluated from the experimental power balance for the H and D plasmas (reproduced from Ref. [38] with the permission of the IOP publishing). The ion heat diffusivities normalized by the gyro-Bohm diffusivity $\chi_{GB(s)}$ (s = H, D) are plotted as well.

Ref. [34] in which it is clearly shown that the TEM turbulent transport decreases with increasing the collisionality as predicted by the estimate using the mixing-length diffusivity. Thus, the reduction of the TEM turbulent transport due to the collisional stabilization effect can be expected for the LHD configuration as well although nonlinear TEM simulations for LHD with different collisionalities still need to be done to get more definite conclusions. Spatial structures of TEM potential fluctuations in H and D plasmas in LHD and the CBC like tokamak are shown in Fig. 9, where regulation of turbulence due to zonal flows is more evident for deuterium plasmas in both LHD and tokamak cases. High-electron-temperature (T_e) LHD plasma experiments relevant for TEM turbulence were done in order to examine the prediction of the GKV simulations as described above [35]. In fact, better high-T_e LHD plasma confinement is experimentally confirmed for D rather than for H, which implies qualitative agreement with the simulation results although further detailed comparisons between simulation and experimental results remain as future tasks.

Experiments of high-T_i isotope plasmas are also done in LHD [36]. In the high-T_i LHD experiments, formations of ion transport barriers (ITBs), where the ion heat transport is significantly reduced, are observed in the core regions of both H and D plasmas although the heat transport and the density fluctuation amplitude are found to be smaller in the D plasma than in the H plasma. Radial profiles of the ion heat diffusivities (χ_i's) evaluated from the experimental power balance for the H and D plasmas are shown in Fig. 10, where the ion heat diffusivities normalized by the gyro-Bohm diffusivity $\chi_{GB(s)}$ (s = H, D) are plotted, as well. Here, $\chi_{GB(s)}$ is defined by $\chi_{GB(s)} \equiv 2^{3/2}\rho_{ts}^2 v_{ts}/R_{ax}$, where $v_{ts} \equiv (T_s/m_s)^{1/2}$ is the thermal velocity, $\rho_{ts} \equiv v_{ts}/\Omega_s$ the gyroradius, $\Omega_s \equiv e_s B_{ax}/(m_s c)$ the gyrofrequency, and R_{ax} (B_{ax}) the major radius (the magnetic field) at the magnetic axis in the vacuum field. It is clearly seen from Fig. 10 that both χ_i and $\chi_i/\chi_{GB(s)}$ are smaller in the D plasma than in the H plasma.

Using the density and temperature profiles obtained from the high-T_i LHD experiments, GKV simulations are carried out for the H and D plasmas [37, 38]. The mixing-length diffusivities for the H and D plasmas are evaluated by $\chi_{ML} \equiv \sum_{k_y}(\gamma/k_y^2)\Delta k_y$, where the growth rate γ is given by the linear GKV simulation as a function of the poloidal wavenumber k_y and Δk_y denotes the non-dimensional minimum grid size in k_y. Figure 11 shows radial profiles of the normalized mixing-length diffusivities, which are qualitatively consistent with the experimental results in Fig. 10 in that the normalized heat diffusivity is reduced in the D plasma. Nonlinear GKV simulations are also performed to obtain the turbulent ion heat diffusivities for the H and D plasmas [37]. The simulations reproduce well the ratio of the ion heat diffusivity in the D plasma to that in the H plasma evaluated from the experimental results although the absolute values of the heat diffusivities are overestimated by the simulations. It is also found from the nonlinear GKV simulations that the ratio of the generated zonal flow energy to the total turbulence energy at the normalized minor radius $\rho \equiv r/a = 0.5$ in the D plasma is about

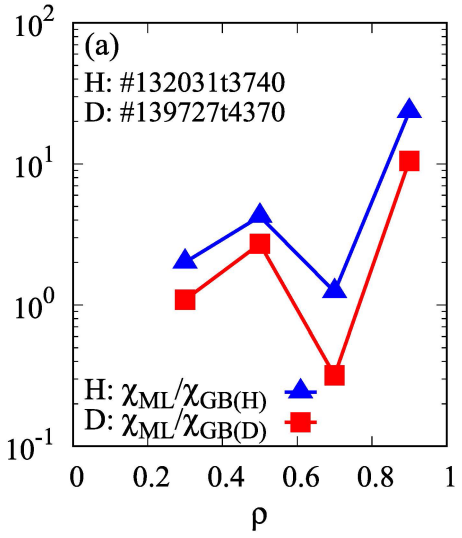

Fig. 11 Radial profiles of the normalized mixing-length diffusivities for the H and D plasmas (reproduced from Ref. [38] with the permission of the IOP publishing).

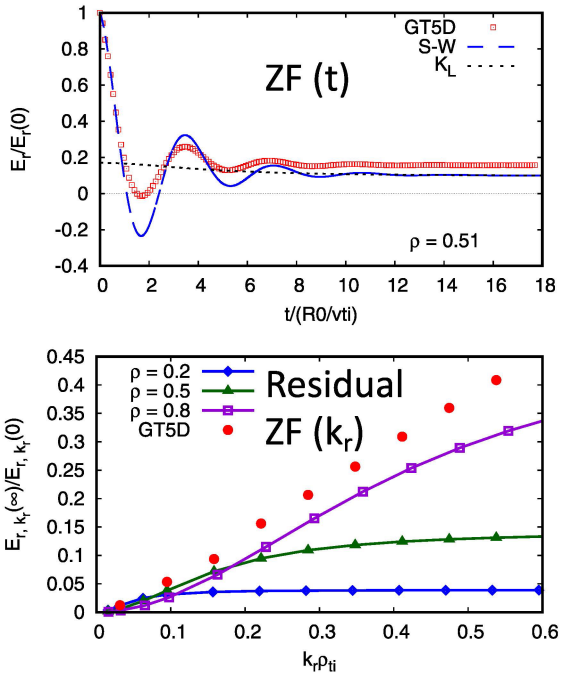

Fig. 12 Time evolutions of GAM oscillations (top) and residual zonal flow levels as functions of the radial wavenumber (bottom) in the LHD configuration obtained from the GT5D simulations and the analytical theory (reproduced from Ref. [51] with the permission of AIP Publishing).

30% larger than that in the H plasma.

The GKV code is also applied to investigate turbulent transport in quasi-axisymmetric systems. The Chinese First Quasi-axisymmetric Stellarator (CFQS) is a joint project of the Southwest Jiaotong University (SWJTU) and NIFS [39, 40]. GKV simulations of linear ITG modes and ITG turbulent transport in the CFQS are performed [41] and their results are compared with those in the equivalent tokamak, which has a circular cross section with the same safety factor q, magnetic shear parameter $\hat{s} = (r/q)(dq/dr)$, and inverse aspect ratio r/R as those of the CFQS. It is found from the linear GKV simulations that the CFQS has wider poloidal wavenumber regions where unstable ITG modes have higher growth rates than those in the equivalent tokamak. However, the nonlinear GKV simulations show that the ITG turbulent heat flux in the CFQS is comparable with or less than the heat flux in the equivalent tokamak, and that the stronger zonal flows are generated in the CFQS. Thus, the quasi-axisymmetric configuration is found to enhance the zonal flow generation and the resultant ITG turbulent transport regulation. The adiabatic-electron approximation is employed in the present nonlinear simulations for the ITG turbulent transport in the CFQS. Effects of kinetic electrons and finite beta on the turbulence are to be examined in the future studies.

Neoclassical transport processes generally make significant contributions to plasma confinement in helical systems more than in tokamaks because radial drift motions of particles trapped in helical magnetic ripples bring about high particle and heat transport fluxes. To investigate transport fluxes, viscosities, radial electric fields, and bootstrap currents produced by neoclassical transport processes in three-dimensional toroidal configurations, global δf Monte Carlo simulation code, FORTEC-3D [42, 43], has been developed and applied to many devices. In non-axisymmetric systems, radial electric fields are determined using the ambipolarity condition for the neoclassical particle fluxes. Thus, FORTEC-3D is used to calculate radial electric field profiles in several helical systems such as LHD [44], TJ-II [45], and W7-X [46], and reasonable agreements between the simulations and the experimental results are confirmed. Also, FORTEC-3D is applied to predict the neoclassical heat flux in the helical demo reactor, FFHR-d1 [47], as well as the neoclassical toroidal viscosity (NTV) in JT-60SA with magnetic perturbations imposed [48, 49].

Developments in global codes aiming at gyrokinetic simulations of turbulent transport processes in helical systems have also started in NSRP. Extension of the global gyrokinetic simulation code (GT5D) to helical geometry is in progress. GT5D is a global full-f gyrokinetic Vlasov simulation code which was developed by Idomura originally for tokamak configurations [50]. Verification studies of the extended version of GT5D are now being done for a typical LHD configuration [51, 52]. Time evolutions of GAM oscillations and residual zonal flow levels as functions of the radial wavenumber in the LHD configuration are shown in Fig. 12, where reasonable agreements between results from the GT5D simulations and the analytical theory [53,54] are verified. Note that GT5D is a full-f code which in principle can simulate both neoclassical and turbulent transport processes. It is verified in Fig. 13 that neoclassical particle fluxes and ambipolar radial radial electric fields calcu-

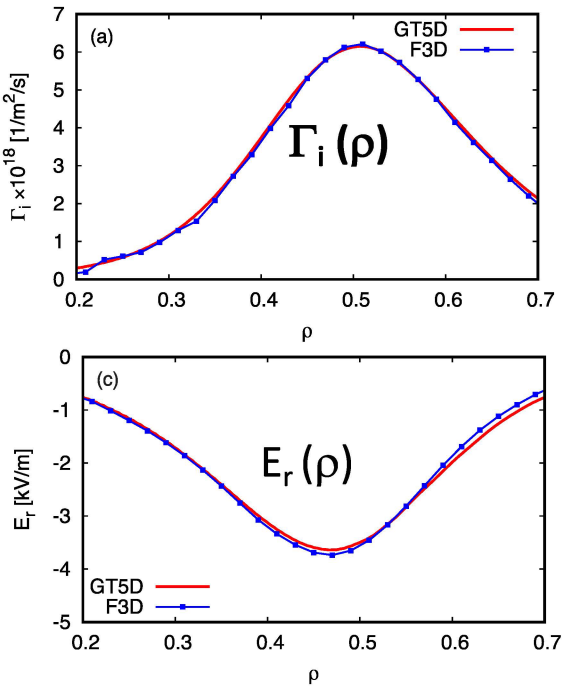

Fig. 13 Radial profiles of neoclassical particle fluxes (a) and ambipolar radial radial electric fields (b) calculated from GT5D and FORTEC-3D codes (reproduced from Ref. [51] with the permission of AIP Publishing).

lated from GT5D are in good agreement with those from FORTEC-3D.

Extension of another global gyrokinetic simulation code (XGC) [55] to helical geometry has been advanced in collaboration between NSRP and Princeton Plasma Physics Laboratory (PPPL) [56]. The X-point included Gyrokinetic Code (XGC) is a global particle-in-cell code which was originally developed by Chang *et al*. [55] to investigate neoclassical and turbulent transport processes in tokamak peripheral plasmas including regions where nested magnetic surfaces do not exist. Benchmark tests of the XGC against the GT5D code and the analytical theory are successfully done for the collisionless damping of GAM oscillations in the LHD configuration. GT5D and XGC global simulations of linear ITG modes and ITG turbulent transport remain as future tasks and comparisons between results from these global simulations and the local GKV simulations are also planned.

Global gyrokinetic simulations are expected to clarify how turbulent particle and heat fluxes are influenced by effects of the global profiles of background densities, temperatures, and radial electric fields, which are difficult for local gyrokinetic simulations to accurately evaluate. Effects of the background radial electric field profile is one of the major concerns from the viewpoint of mechanisms for improving plasma confinement. We note here that, for the helical system with the background radial electric field E_r, the formula of the residual zonal flow potential $\phi(\infty)$ in the long time limit after the collisionless damping process is theoretically derived [57] as

$$\phi(\infty) = \frac{\phi(0)}{1 + G_p + G_t + M_p^{-2}(G_{ht} + G_h)(1 + T_e/T_i)}, \tag{1}$$

where $\phi(0)$ are the zonal flow potential in the long time limit and that at the initial time, respectively, the dimensionless geometrical factors G_p, G_t, G_{ht}, and G_h are defined in Ref. [57], and $M_p \equiv |(v_E/r)(Rq/v_{ti})|$ represents the poloidal Mach number defined with the background $\mathbf{E} \times \mathbf{B}$ drift velocity $v_E \equiv cE_r/B_0$, the ion thermal velocity $v_{ti} \equiv (T_i/m_i)^{1/2}$, the safety factor q, and the minor (major) radius r (R). The validity of Eq. (1) is verified by the linear GKV simulation using multi-flux-tubes distributed over a given flux surface [58]. Since the poloidal Mach number M_p is proportional to the product of the background radial electric field and the square root of the ion mass, the heavier ion mass gives the larger Mach number and the higher residual zonal flow level according to the formula shown in Eq. (1). Thus, the favorable effect on the turbulent transport regulation due to the hydrogen isotopes with heavier mass is expected, and it is one of the interesting subjects for GT5D and XGC global simulations to focus on in the future.

Gyrokinetic turbulent transport simulations described above are regarded as being based on the rigorous first-principle model although they generally require huge computer resources. However, for the purpose of application to a large number of transport analyses for experimental results and reactor designs, it is desirable to perform simulations using simpler transport models with lower computational costs than the direct gyrokinetic turbulence simulations. In NSRP, turbulent transport models, which can quickly reproduce results from nonlinear gyrokinetic simulations of turbulent transport in helical systems, have been studied. Based on the GKV turbulence simulation results, the model formula for the ion heat diffusivity χ_i in the ITG turbulence is derived [59] as

$$\frac{\chi_i^{\mathrm{model}}}{\chi_i^{\mathrm{GB}}} = \frac{A_1(\sum_k \tilde{\gamma}_k/\tilde{k}_y^2)^\alpha}{A_2 + \tilde{\tau}_{\mathrm{ZF}}/(\sum_k \tilde{\gamma}_k/\tilde{k}_y^2)^{1/2}}, \tag{2}$$

where $A_1 \equiv 1.8 \times 10^1$ and $A_2 \equiv 5.2 \times 10^{-1}$ are the dimensionless coefficients, $\tilde{k}_y \equiv k_y \rho_{ti}$ the normalized poloidal wavenumber, $\tilde{\gamma}_k \equiv \gamma_k/(v_{ti}/R)$ the normalized wavenumber-dependent ITG mode growth rate, and $\tilde{\tau}_{\mathrm{ZF}} \equiv \tau_{\mathrm{ZF}}/(R/v_{ti})$ the normalized linear ZF response time [see Ref. [59] for details].

The χ_i model in Eq. (2) can well predict the nonlinear GKV simulation results, and it is applied to the integrated transport code (TASK3D) [60] which is found to successfully simulate the T_i profile in the high-T_i LHD experiment [61]. Extension of the χ_i model is also done to include effects of trapped electrons on the ITG turbulent transport in the LHD plasmas [62]. In addition, quasilinear models for the ion energy flux, the electron energy flux,

and the particle flux are newly constructed for the case of the ITG turbulence including effects of trapped electrons, for which reasonable agreements between the quasilinear flux models and the nonlinear GK simulations are verified [63]. However, further extension of these models and their validation for the case of the TEM turbulent transport as shown in Fig. 8 remain as future tasks. These new models will be applied to transport simulations predicting profiles of T_i, T_e, and n_e (the electron density) in the LHD plasmas.

At the end of this section, we note recent progress in the development of the integrated transport analysis suite, TASK3D [60]. As for the LHD experiment analysis version (TASK3D-a), it has been further extended by improving the NBI module to be applicable to H/D/He mixture plasmas, realizing loose coupling to the local neoclassical transport code (DKES/PENTA) [64, 65] with the momentum conservation correction technique [66], and implementing the modules for analyzing energetic particles. These extensions are targeted to the LHD deuterium experiments and facilitate database creation for researches on key issues such as energy transport and hydrogen isotope effects. Exploiting such accumulated database by TASK3D-a, thermal transport modeling are made through statistical analyses and neural network approaches. Data assimilation methods are also employed for the integrated predictive modeling in collaboration with Kyoto University. Modules from TASK3D-a are continuously utilized for core plasma designs for the the helical demo reactor, FFHR [47, 67].

4. Studies on Basic Physical Processes and Simulation Science Basis Technologies

In NSRP, simulation studies on basic physical processes in plasmas and researches on simulation science basis technologies are actively progressed as highlighted in this section. By means of particle simulations which mimic merging plasmas in a spherical tokamak (ST), ion heating processes during magnetic reconnection in the presence of a guide toroidal magnetic field are studied [68–72]. Simulation results in Fig. 14 show that a circle- or an arc-shape ion velocity distribution is formed in the downstream, which implies that ions are effectively heated. In addition, the simulation results reproduce tendencies observed in ST experiments, for example, the dependence of the ion temperature on the toroidal magnetic field.

Simulations of complex processes caused by plasma-wall interactions are also carried out in NSRP. It was found in the experimental device NAGDIS-II at Nagoya University that the low energy helium plasma irradiation on the tungsten (W) surface produces fuzz nanostructures [73, 74]. In order to investigate mechanisms of the tungsten fuzz formation composed of the multi-scale and multi-physics processes, the multi-hybrid simulation method has been developed [75, 76]. In the multi-hybrid simulation, the irradiation process of the helium (He) plasma onto the W surface is solved by the binary collision approximation (BCA), the diffusion process of the He atoms in the W material is treated by the random-walk model based on kinetic Monte-Carlo (KMC), and the deformation process of the W material due to the pressure from the helium bubble is simulated by the molecular dynamics (MD). The BCA-MD-KMC simulation elucidates the process in which the tungsten fuzz is grown by the He bubble agglomeration.

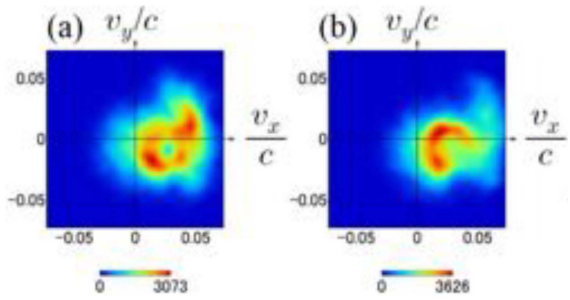

Fig. 14 Ion velocity distributions formed in the downstream from the reconnection region.

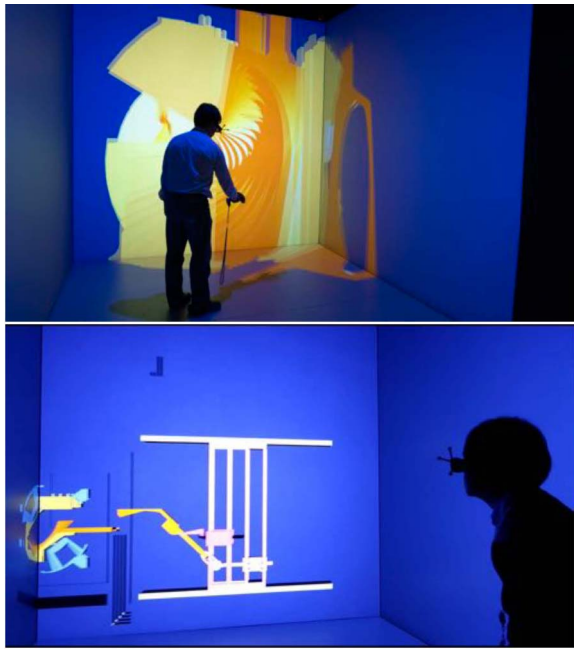

Fig. 15 Application of Virtual-Reality (VR) to the fusion engineering. The viewer grasps the component by his virtual hand (top). The viewer watches the movement of component by the robot system (bottom).

As an example of research activities in the science basis technologies, application of the Virtual-Reality (VR) to the fusion engineering is advanced in NSRP [77, 78]. The VR technology is expected to play important roles in the design, construction, and maintenance of the fusion reactor. Also, the robotics system will perform regularly the maintenance, such as component replacement. Then, it is

not easy to determine how to move and rotate the components on the 2D monitor by using the CAD software because the information regarding depth is lost. We can seek the efficient assembly and replacement procedures by investigating the component movements including the robot motion in the VR space. Such examples of the VR application are shown in Fig. 15.

5. Summary

In this article, recent progress in the Numerical Simulation Reactor Research Project (NSRP) is presented. NSRP is promoting large-scale numerical simulation researches through close collaborations with experimental and engineering groups aiming at realization of Numerical Helical Reactor, which is an integrated system of simulation codes to predict behaviors of fusion plasmas over the whole machine range. To construct reliable simulation codes which can make accurate predictions, verification and validation (V&V) studies are actively carried out based on comparisons among improved theoretical models, simulation results, and experimental observations in tokamaks and helical devices.

Highlighted topics are successful accomplishments recently made by the following studies: (i) MEGA code simulations of the EP-driven Alfvén eigenmodes, fast-ion transport, EGAMs, bulk-ion heating, and kinetic effects on the RBM, (ii) FORTEC-3D code simulations of neoclassical transport, ambipolar radial electric fields, neoclassical toroidal viscosities due to resonant magnetic perturbations, (iii) GKV code simulations of the ITG and TEM turbulent transport, zonal flows, and isotope effects, (iv) the benchmark tests of the global gyrokinetic codes (GT5D and XGC) regarding neoclassical transport and zonal flow damping in the LHD configuration, (v) modeling of turbulent transport by the turbulent ion heat diffusivity and by the quasilinear fluxes of particles and energies for ions and electrons, (vi) development of the integrated transport code (TASK3D) (vii) particle simulations of the effective ion heating through merging plasmas in a spherical tokamak, (viii) multi-hybrid (BCA-MD-KMC) simulations of fuzz nanostructures on a tungsten surface irradiated by a helium plasma, and (ix) application of the virtual-reality (VR) technology to the fusion engineering. Not all activities in NSRP are covered in this article due to the space limitation although part of recent NSRP results which are not shown here are presented in Refs. [79–92].

As future plans, NSRP promotes further extensions of the various simulation codes, developments of the integrated code system, and their V&V studies based on LHD deuterium experiments and other device experiments to tackle key issues such as energetic particle confinement, kinetic effects on MHD stability, isotope effects on turbulence, impurity transport in core and peripheral plasmas, and plasma-wall interactions. NSRP will thus make significant contributions to plasma confinement improvement, optimization of configuration for high plasma performance, and reactor design through further advancing domestic and international collaborations.

Acknowledgments

The author (HS) deeply thanks the International Program Committee of the 27th International Toki Conference on Plasma and Fusion Research and the 13th Asia Pacific Plasma Theory Conference for giving him the opportunity of the plenary presentation which has lead to this Overview article. Support from all collaborators in the National Institute for Fusion Science (NIFS), other institutes, and universities to the Numerical Simulation Reactor Research Project (NSRP) is highly appreciated. Numerical simulations were carried out with the use of the Plasma Simulator and the LHD Numerical Analysis System at NIFS.

[1] R. Horiuchi, J. Plasma Fusion Res. **90**, 2 (2014) (in Japanese).
[2] R. Horiuchi, J. Plasma Fusion Res. **92**, 785 (2016) (in Japanese).
[3] Y. Takeiri *et al.*, Nucl. Fusion **57**, 102023 (2017).
[4] A. Sagara *et al.*, Nucl. Fusion **57**, 086046 (2017).
[5] K. Ichiguchi *et al.*, J. Plasma Fusion Res. **92**, 787 (2016) (in Japanese).
[6] Y. Todo *et al.*, J. Plasma Fusion Res. **92**, 806 (2016) (in Japanese).
[7] M. Yokoyama, J. Plasma Fusion Res. **92**, 814 (2016) (in Japanese).
[8] R. Kanno *et al.*, J. Plasma Fusion Res. **92**, 794 (2016) (in Japanese).
[9] Y. Suzuki *et al.*, J. Plasma Fusion Res. **92**, 810 (2016) (in Japanese).
[10] S. Ishiguro *et al.*, J. Plasma Fusion Res. **92**, 821 (2016) (in Japanese).
[11] Y. Todo, Phys. Plasmas **13**, 082503 (2006).
[12] Y. Todo *et al.*, Plasma Fusion Res. **9**, 3403068 (2014).
[13] Y. Todo *et al.*, Nucl. Fusion **55**, 073020 (2015).
[14] A. Bierwage *et al.*, Nature Comm. **9**, 3281 (2018).
[15] Y. Hu *et al.*, Phys. Plasmas **23**, 022505 (2016).
[16] T.L. Rhee *et al.*, 11th Asian Pacific Plasma Theory Conference (Jeju, Korea, 2014), P26.
[17] J. Gonzalez-Martin *et al.*, 45th European Physical Society Conference on Plasma Physics (Prague, Czech Republic, 2018), I5.013.
[18] Y. Todo *et al.*, Phys. Plasmas **24**, 081203 (2017).
[19] P. Adulsiriswad *et al.*, 60th Annual Meeting of the APS Division of Plasma Physics (Portland, USA, 2018), PP11.00068.
[20] Y. Todo *et al.*, Nucl. Fusion **56**, 112008 (2016).
[21] Y. Todo, 27th IAEA Fusion Energy Conference, (Ahmedabad, India, 2018), TH/1-2.
[22] Y. Todo, 27th International Toki Conference on Plasma and Fusion Research and 13th Asia Pacific Plasma Theory Conference (Toki, Japan, 2018), P1-38.
[23] K.L. Wong *et al.*, Phys. Rev. Lett. **66**, 1874 (1991).
[24] H. Wang *et al.*, Phys. Rev. Lett. **120**, 175001 (2018).
[25] T. Ido *et al.*, Phys. Rev. Lett. **116**, 015002 (2016).
[26] H. Wang *et al.*, 27th IAEA Fusion Energy Conference, (Ahmedabad, India, 2018), TH/P2-11.
[27] H. Wang *et al.*, 27th International Toki Conference on

Plasma and Fusion Research and 13th Asia Pacific Plasma Theory Conference (Toki, Japan, 2018), O-3.
[28] M. Sato *et al.*, 27th IAEA Fusion Energy Conference, (Ahmedabad, India, 2018), TH/P5-25.
[29] T.-H. Watanabe *et al.*, Nucl. Fusion **46**, 24 (2006).
[30] M. Nakata *et al.*, Nucl. Fusion **58**, 074008 (2016).
[31] M. Nunami *et al.*, Phys. Plasmas **19**, 042504 (2012).
[32] A. Ishizawa *et al.*, Nucl. Fusion **55**, 043024 (2015).
[33] M. Nakata *et al.*, Plasma Phys. Control. Fusion **61**, 014016 (2016).
[34] M. Nakata *et al.*, Phys. Rev. Lett. **118**, 165002 (2017).
[35] K. Tanaka *et al.*, 27th IAEA Fusion Energy Conference, (Ahmedabad, India, 2018), EX/P3-6.
[36] K. Nagaoka *et al.*, 27th IAEA Fusion Energy Conference, (Ahmedabad, India, 2018), EX/5-1.
[37] M. Nakata *et al.*, 45th European Physical Society Conference on Plasma Physics (Prague, Czech Republic, 2018), I2.105.
[38] M. Nakata *et al.*, Plasma Phys. Control. Fusion **61**, 014016 (2019).
[39] H. Liu *et al.*, Plasma Fusion Res. **13**, 3405067 (2018).
[40] M. Isobe *et al.*, 27th International Toki Conference on Plasma and Fusion Research and 13th Asia Pacific Plasma Theory Conference (Toki, Japan, 2018), P1-41.
[41] M. Nakata *et al.*, 27th International Toki Conference on Plasma and Fusion Research and 13th Asia Pacific Plasma Theory Conference (Toki, Japan, 2018), O-1.
[42] S. Satake *et al.*, Plasma Fusion Res. **3**, S1062 (2008).
[43] S. Satake *et al.*, 2nd Asia-Pacific Conference on Plasma Physics (Kanazawa, Japan, 2018), MFP-41.
[44] N. A. Pablant *et al.*, Plasma Phys. Control. Fusion **58**, 045004 (2016).
[45] F. Sánchez *et al.*, Nucl. Fusion **55**, 104014 (2015).
[46] N. A. Pablant *et al.*, Phys. Plasmas **25**, 022508 (2018).
[47] T. Goto *et al.*, Nucl. Fusion **57**, 066011 (2017).
[48] S. Satake *et al.*, Phys. Rev. Lett. **107**, 055001 (2011).
[49] M. Honda *et al.*, Nucl. Fusion **58**, 112012 (2011).
[50] Y. Idomura *et al.*, Comput. Phys. Commun. **179**, 391 (2008).
[51] S. Matsuoka *et al.*, Phys. Plasmas **25**, 022510 (2018).
[52] S. Matsuoka *et al.*, 2nd Asia-Pacific Conference on Plasma Physics (Kanazawa, Japan, 2018), O-1.
[53] H. Sugama *et al.*, Phys. Rev. Lett. **94**, 115001 (2005).
[54] H. Sugama *et al.*, Phys. Plasmas **13**, 012501 (2006).
[55] C.S. Chang *et al.*, Nucl. Fusion **57**, 116023 (2017).
[56] T. Moritaka *et al.*, 27th IAEA Fusion Energy Conference, (Ahmedabad, India, 2018), TH/P5-5.
[57] H. Sugama *et al.*, Phys. Plasmas **16**, 056101 (2009).
[58] T.-H. Watanabe *et al.*, Nucl. Fusion **51**, 123003 (2011).
[59] M. Nunami *et al.*, Phys. Plasmas **20**, 092307 (2013).
[60] M. Sato *et al.*, Plasma Fusion Res. **3**, S1063 (2008).
[61] S. Toda *et al.*, J. Phys.: Conf. Ser. **561**, 012020 (2014).
[62] S. Toda *et al.*, Plasma Fusion Res. **12**, 1303035 (2017).
[63] S. Toda *et al.*, 2nd Asia-Pacific Conference on Plasma Physics (Kanazawa, Japan, 2018), B-I46.
[64] P. Hirshman *et al.*, Phys. Fluids **29**, 2951 (1986).
[65] D.A. Spong, Phys. Plasmas **12**, 056114 (2005).
[66] H. Sugama *et al.*, Phys. Plasmas **9**, 4637 (2002).
[67] T. Goto *et al.*, 27th International Toki Conference on Plasma and Fusion Research and 13th Asia Pacific Plasma Theory Conference (Toki, Japan, 2018), I-03.
[68] S. Usami *et al.*, Phys. Plasmas **23**, 092101 (2017).
[69] S. Usami *et al.*, Plasma Fusion Res. **13**, 3401025 (2018).
[70] S. Usami *et al.*, 27th IAEA Fusion Energy Conference, (Ahmedabad, India, 2018), TH/P4-9.
[71] S. Usami *et al.*, 2nd Asia-Pacific Conference on Plasma Physics (Kanazawa, Japan, 2018), F-I15.
[72] S. Usami *et al.*, 27th International Toki Conference on Plasma and Fusion Research and 13th Asia Pacific Plasma Theory Conference (Toki, Japan, 2018), P2-66.
[73] S. Takamura *et al.*, Plasma Fusion Res. **1**, 051 (2006).
[74] S. Kajita *et al.*, J. Nucl. Mater. **418**, 152 (2011).
[75] A.M. Ito *et al.*, 2nd Asia-Pacific Conference on Plasma Physics (Kanazawa, Japan, 2018), MF-I43.
[76] A.M. Ito *et al.*, 27th International Toki Conference on Plasma and Fusion Research and 13th Asia Pacific Plasma Theory Conference (Toki, Japan, 2018), P2-50.
[77] H. Ohtani *et al.*, 2nd Asia-Pacific Conference on Plasma Physics (Kanazawa, Japan, 2018), B-I3.
[78] H. Ohtani *et al.*, 27th International Toki Conference on Plasma and Fusion Research and 13th Asia Pacific Plasma Theory Conference (Toki, Japan, 2018), P2-75.
[79] R. Kanno *et al.*, 27th International Toki Conference on Plasma and Fusion Research and 13th Asia Pacific Plasma Theory Conference (Toki, Japan, 2018), P1-15.
[80] G. Kawamura *et al.*, 27th International Toki Conference on Plasma and Fusion Research and 13th Asia Pacific Plasma Theory Conference (Toki, Japan, 2018), P1-22.
[81] S. Toda *et al.*, 27th International Toki Conference on Plasma and Fusion Research and 13th Asia Pacific Plasma Theory Conference (Toki, Japan, 2018), P1-26.
[82] S. Satake *et al.*, 27th International Toki Conference on Plasma and Fusion Research and 13th Asia Pacific Plasma Theory Conference (Toki, Japan, 2018), P1-30.
[83] S. Ishiguro *et al.*, 27th International Toki Conference on Plasma and Fusion Research and 13th Asia Pacific Plasma Theory Conference (Toki, Japan, 2018), P1-67.
[84] H. Miura *et al.*, 27th International Toki Conference on Plasma and Fusion Research and 13th Asia Pacific Plasma Theory Conference (Toki, Japan, 2018), P2-01.
[85] K. Ichiguchi *et al.*, 27th International Toki Conference on Plasma and Fusion Research and 13th Asia Pacific Plasma Theory Conference (Toki, Japan, 2018), P2-03.
[86] N. Mizuguchi *et al.*, 27th International Toki Conference on Plasma and Fusion Research and 13th Asia Pacific Plasma Theory Conference (Toki, Japan, 2018), P2-03.
[87] M. Toida *et al.*, 27th International Toki Conference on Plasma and Fusion Research and 13th Asia Pacific Plasma Theory Conference (Toki, Japan, 2018), P2-12.
[88] H. Hasegawa *et al.*, 27th International Toki Conference on Plasma and Fusion Research and 13th Asia Pacific Plasma Theory Conference (Toki, Japan, 2018), P2-25.
[89] Y. Suzuki *et al.*, 27th International Toki Conference on Plasma and Fusion Research and 13th Asia Pacific Plasma Theory Conference (Toki, Japan, 2018), P2-26.
[90] K. Fujita *et al.*, 27th International Toki Conference on Plasma and Fusion Research and 13th Asia Pacific Plasma Theory Conference (Toki, Japan, 2018), P2-37.
[91] A. Takayama *et al.*, 27th International Toki Conference on Plasma and Fusion Research and 13th Asia Pacific Plasma Theory Conference (Toki, Japan, 2018), P2-51.
[92] H. Nakamura *et al.*, 27th International Toki Conference on Plasma and Fusion Research and 13th Asia Pacific Plasma Theory Conference (Toki, Japan, 2018), P2-59.